

Compressively Sensed Image Recognition

Ayşen Değeri¹, Sinem Aslan^{2,3}, Mehmet Yamaç¹, Bülent Sankur⁴, and Moncef Gabbouj¹

¹Tampere University of Technology, Laboratory of Signal Processing, Tampere, Finland

²Ca' Foscari University of Venice, European Centre for Living Technology, Venice, Italy

³Ege University, International Computer Institute, İzmir, Turkey

⁴Boğaziçi University, Electrical and Electronics Engineering Department, İstanbul, Turkey

Abstract—Compressive Sensing (CS) theory asserts that sparse signal reconstruction is possible from a small number of linear measurements. Although CS enables low-cost linear sampling, it requires non-linear and costly reconstruction. Recent literature works show that compressive image classification is possible in CS domain without reconstruction of the signal. In this work, we introduce a DCT base method that extracts binary discriminative features directly from CS measurements. These CS measurements can be obtained by using (i) a random or a pseudo-random measurement matrix, or (ii) a measurement matrix whose elements are learned from the training data to optimize the given classification task. We further introduce feature fusion by concatenating Bag of Words (BoW) representation of our binary features with one of the two state-of-the-art CNN-based feature vectors. We show that our fused feature outperforms the state-of-the-art in both cases.

Index Terms—Compressive Sensing, Compressive Learning, Inference on Measurement Domain, Learned Measurement Matrix, Compressive Classification, DCT-based Binary Descriptor.

I. INTRODUCTION

The first step in any signal processing task is the acquisition of signals. The classical pathway for band-limited signals is to instantaneously sample the signal at the Nyquist-Shannon rate, then compress the signal to remove redundancies and/or irrelevancies, typically using a transform-based compression technique for efficient storage and transmission. The compressed signal must be decompressed before executing any further signal processing operation such as classification, detection, inference. etc.

The new sampling paradigm, *Compressive Sensing (CS)* [1] bypasses this laborious Nyquist-Shannon data acquisition scheme in that signals are being compressed while being sampled with random patterns. Thus the sampling and compression steps are combined into one action. However, the reconstruction of the signal from *compressively sensed measurements (CSMs)* becomes non-linear and considerably costlier in the computational effort. This costly signal reconstruction operation would be counterproductive were it not for the emerging signal processing algorithms in the compressed domain. A newly emerging idea [2]–[4] is using CSMs directly in inference problems without executing any reconstruction. This promising approach can potentially be advantageous in real-time applications and/or when dealing with big data.

In a pioneering work, Davenport et al. [4] have addressed the problem of inference directly on compressively sensed

measurements. In [5], it is theoretically shown that the accuracy of the soft margin SVM classifier is preserved when data is collected with sparse random projections. The authors in [6] have introduced the idea of smashed filter and, based on the Johnson-Lindenstrauss Lemma [7] have shown that the inner product of two signals is relatively preserved for compressively sampled signals when the sampling matrix consists of random values, chosen from some specific probability distributions. Different versions of the smashed filter are used in various applications [8], [9]. For instance in [9], a compressive smashed filter technique is proposed by first producing a set of correlation filters from uncompressed images in the training set, and then at the testing stage by correlating CSMs of test images and with the CSMs of learned filters. A linear feature extraction method in CS domain is developed in [10] for direct classification of compressively sensed EEG data. In [11] fed an SVM classifier with a fusion of CSMs (projected data) and dynamic features and they reported performance beyond the state-of-the-art for 1-D ECG data classification.

Other works, e.g., [12], [13], have provided theoretical guarantees for achievable accuracy in different CSM setups for both sparse and non-sparse cases.

All the above works try to use compressed samples directly to solve the inference problem. A second approach is to boost the size of CSMs to the original image size by a simple linear projection, but avoiding the costly nonlinear reconstruction procedure. This simple back-projection yields a pseudo-image and one then proceeds with the inference task on this imperfectly reconstructed image. This image, restituted to its original dimension and also known as *proxy image*, is usually a heavily degraded version of the original image. One way to obtain the proxy image is by premultiplying the compressed image by the transpose of the sampling matrix. In [14], the authors apply a CNN-based feature extraction method on such a proxy image. Their measurement matrix consists of random Gaussian distributed numbers. Another work [15] uses a deeper network structure (as compared to [14]) by adding two fully connected layers at the beginning of the network. Thus this network can learn as well the linear dimension reduction (so-called measurement matrix) and linear back projection to the image domain (i.e., the transpose of the measurement matrix).

In this work, following the vein of the second approach we propose a DCT-based discriminative feature scheme, computed

directly from the proxy image. This feature vector (called MB-DCT) is binary, hence simple and low cost. A preliminary version of this feature was presented in EUSIPCO [16]. In this work, we applied MB-DCT on non-compressively sampled images. In [16] we had shown that this simple scheme of selected binarized DCT coefficients, computed in increasing scales of local windows was remarkably robust against linear and nonlinear image degradations, such as additive white Gaussian noise, contrast and brightness changes, blurring, and strong JPEG compression. We use MB-DCT scheme in [16] for feature extraction from image proxies. Our experimental results show that using this simple binary feature method surpasses the performance of Smashed Filters [9]. We further introduce feature fusion by concatenating Bag of Words (BoW) representation of our binary features with one of the two state-of-the-art CNN-based feature vectors, i.e., in [14] and [15]. In the method [14], elements of measurement matrices were drawn from a random distribution as typical in conventional CS theory, whereas in the method [15] sampling matrices were learned from a deep network; the latter method proved to be superior for smaller measurement rates. However, random sensing scheme may still be needed for some applications where one needs to pre-classify the data directly using CSMs, then reconstruct the signal for further analysis. For instance in a remote health monitoring system, we may wish to detect anomalies directly from CSMs of ECG signal on the sensor side. Then based on the sensor side classification, CSMs of selected cases can be transmitted for a more detailed analysis by a medical doctor. Therefore, we consider the random sensing approach and learned sensing approach as two different set-ups. In this paper, we show that our fused features outperforms the aforementioned works for both of the schemes and gives the state-of-the-art performance.

We briefly introduce the notation used and some preliminary information. We define the ℓ_0 -norm of the vector $x \in \mathbb{R}^N$ as $\|x\|_{\ell_0} = \lim_{p \rightarrow 0} \sum_{i=1}^N |x_i|^p = \#\{j : x_j \neq 0\}$. The compressive sensing (CS) scheme extracts m number of measurements from the N -dimensional input signal $S \in \mathbb{R}^N$, i.e.,

$$y = \Psi S, \quad (1)$$

where Ψ is the $m \times N$ measurement matrix and typically $m \ll N$. Consider this signal to be k -sparse in a sparsifying basis Φ such that $S = \Phi x$ with $\|x\|_{\ell_0} \leq k$. Then, the general compressive sensing setup is

$$y = \Psi \Phi x = Ax, \quad (2)$$

where $A = \Psi \Phi$ is sometimes called as holographic matrix. It has been demonstrated that the sparse representation in (3) is unique if $m \geq 2k$ [17].

$$\min_x \|x\|_{\ell_0} \quad \text{subject to } Ax = y \quad (3)$$

The organization of the rest of the paper is as follows. In Section II, we provide the notation, mathematical foundations and a brief review of CS theory. The difference between the two measurement approaches, namely, based random weights

or learned weights in the acquisition of CSMs and reconstruction of proxies are explained in Section III. Then in Section IV, we introduce the proposed feature extraction method from the two proxy varieties. Finally, performance evaluations of the proposed method are given and a conclusion is drawn.

II. RELATED WORKS

The signal reconstruction expounded in (3) is an NP-hard problem. Among the plethora of methods to overcome the computational impasse one can list convex relaxation, various greedy algorithms, Bayesian framework, non-convex optimization, iterative thresholding methods etc. [18]. However, these algorithms still suffer from computational complexity and must be restricted mostly to non-real time applications. For an application where a fast and real-time data inference is required, one possible solution could be designing a non-iterative solution such as a simple forward pass re-constructor [19], [20] based on neural networks. These types of solutions, nevertheless, remain still wasteful of resources since we have to return to the high-dimensional ambient domain from the compressed domain in order to execute tasks such as feature extraction, classification etc. Furthermore the exact recovery probability, that is the phase diagram of the recovery algorithms, depends critically on the sparsity level k and the number of measurements, m [21]. When the proportion of measurements is very low, typically for $\frac{m}{N} \leq 0.1$ most reconstruction algorithms fail. Approaches to tackle the reconstruction bottleneck have been to bypass the reconstruction step altogether, and make inferences directly on the sparse signal y [9], or on some proxy of the signal, $\tilde{S} = \Psi^T y$ without solving the inverse problem for sparse reconstruction \hat{x} as in Eq. (3), therefore $\tilde{S} = \Phi \hat{x}$, where \tilde{S} full recovery of the vectorized image. We can express the linear degradation on the proxy as

$$\tilde{S} = \Psi^T y = \Psi^T \Psi S = HS, \quad (4)$$

where $H = \Psi^T \Psi$ is a non-invertible matrix that represents the non-linear degradation on original signal S .

A. Feature extraction from compressively sensed signals with random measurement matrices

In order to guarantee the exact recovery of the k -sparse signal x from y , the measurement matrix Ψ should satisfy certain properties. For example, the measurement matrix, Ψ with i.i.d. elements $\Psi_{i,j}$ drawn according to $\mathcal{N}(0, \frac{1}{m})$, and $m > k(\log(N/k))$ guarantees with high probability the exact signal reconstruction when we relax the ℓ_0 to ℓ_1 in (3) [22]. Random measurement matrices are known to be universally optimum in the sense that they are data independent of characteristics of the data, and they satisfy minimum reconstruction error with minimum m when we do not have another prior information about k -sparse signal. The acquisition of the proxy signal is obviously done as, $\tilde{S} = \Psi^T y$, where $\Psi^T \in \mathbb{R}^{N \times m}$ is the transpose of the measurement matrix Ψ . An example proxy image is shown in Figure 1.

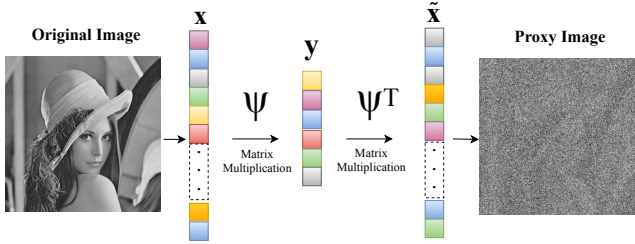


Fig. 1: The image of Lena and its proxy $\Psi^T y$ obtained from CSMs, where y results from projecting the original image on a Gaussian random measurement matrix.

B. Feature extraction from compressively sensed signals based on measurement matrices with learned coefficients

Design of optimal measurement matrices for CS reconstruction and/or for inference tasks is an active research area. An approach to learn a projection operator from image to measurement domain and its backprojection operator from compressed domain to image domain is presented in [14]. The authors have used two fully-connected layers that are followed by convolution layers. The first layer takes the original image S and projects it to the measurement domain, y . The learned weights of this layer represent the elements of measurement matrix for compressively sensing images. The second layer represents the back projection to the image domain to produce a proxy of the image, i.e., $\tilde{S} = \tilde{\Psi}^T y$. In this expression $\tilde{\Psi}^T$ is the learned transpose of the measurement matrix, which is used instead of the transpose of the true measurement matrix, Ψ^T . The output of this layer, the proxy image, is given as input to convolutional layers to realize some non-linear inference task, e.g., classification. Thus the measurement matrix, the pseudo-transpose of the measurement matrix and convolutional network are all jointly learned from the training data. Figure 2 illustrates the first two fully-connected layers of this network.

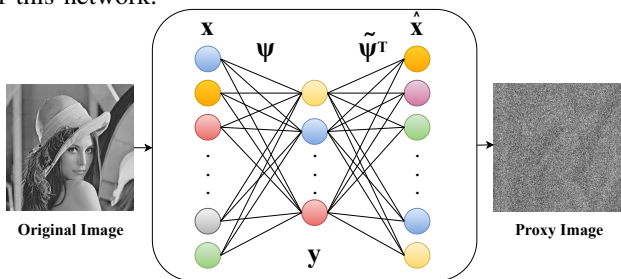


Fig. 2: An original image and its proxy $\Psi^T y$ where y that is obtained using the learned measurement matrix.

III. PROPOSED APPROACH

In this work, we have employed MB-DCT features extracted from proxy images (see Eq. 4) for classification tasks. Specifically, we applied the MB-DCT of [16] as follows: i) we use 4 window scales (instead of 6 as in [16]) and the size of the largest window is now 24 pixels instead of 128 pixels [16]) to fit smaller sized MNIST images (28×28 pixels);

ii) we apply a different scheme of coefficient elimination in that we keep the best performing of the three sets (based on AC energy preservation) of DCT coefficients in the sense of classification accuracy. An MB-DCT descriptor consists of mean quantization of 2D-DCT transform coefficients as computed from multiscale blocks around (densely or sparsely chosen) image points [16].

We employ the mentioned scheme of MB-DCT features in two main modes: 1) The conventional BoW framework as in [16]; 2) A fusion scheme where MB-DCT features are complemented with deep learning features.

A. MB-DCT

We review briefly the MB-DCT features:

(1) *DCT computation*: 2D-DCT coefficients are computed in multiple nested blocks around selected image points, each incrementally changing in size. Similar to [16], we employ various sized windows in this work, in order to capture contextual information in different sized neighbourhoods around every image point. We compute 2D-DCT in four scales corresponding to block sizes $\{8, 12, 16, 24\}$, which seemed adequate for 28×28 pixel-sized MNIST images. For larger images, larger block sizes can be investigated for performance-computational cost tradeoff.

(2) *Eliminating irrelevant coefficients*: A subset of zig-zag ordered DCT coefficients are kept for each block as features and the remaining coefficients are eliminated as irrelevant. The DC term was discarded in all scales as in [16], which also desensitizes the feature vectors to illumination level. We experimented for different sized subsets of the zig-zag ordered coefficients in each scale. Specifically, to determine the quantity of DCT coefficients kept, we start with a random subset of training images. Then, we find three sets of zig-zag ordered DCT coefficients for every pixel location preserving, respectively, 90% and 95% of the AC energy. We repeat this experiment for each scale and for each window size. Finally, we fix the number of coefficients for each energy level (and for each scale) to the average, over all training images, number of coefficients that have met energy preservation percentages. For 100% of the energy preservation we keep all the AC coefficients. For the window sizes of $\{8, 12, 16, 24\}$, we found that the average number of AC coefficients corresponding to 90% and 95% energy are $\{15, 26, 37, 73\}$ and $\{21, 40, 63, 130\}$, respectively. Using these sets of coefficients specific to the window size, we measured the classification error rate on MNIST proxy images at different sensing rates. The resulting error rates are given in Table 1, where one can see that the performances do not differ significantly. Notice that one needs to use quite larger set of coefficients as compared to when original images were used [16]. Due to the imperfect reconstruction of proxy images, the structural information in the image is not as compact as in the original one.

(3) *Binarization of the coefficients*: Since binary features are memory and computation efficient, we binarized the selected coefficients of each block by mean quantization similar to [16]. We also tried median quantization and also trimming, but the

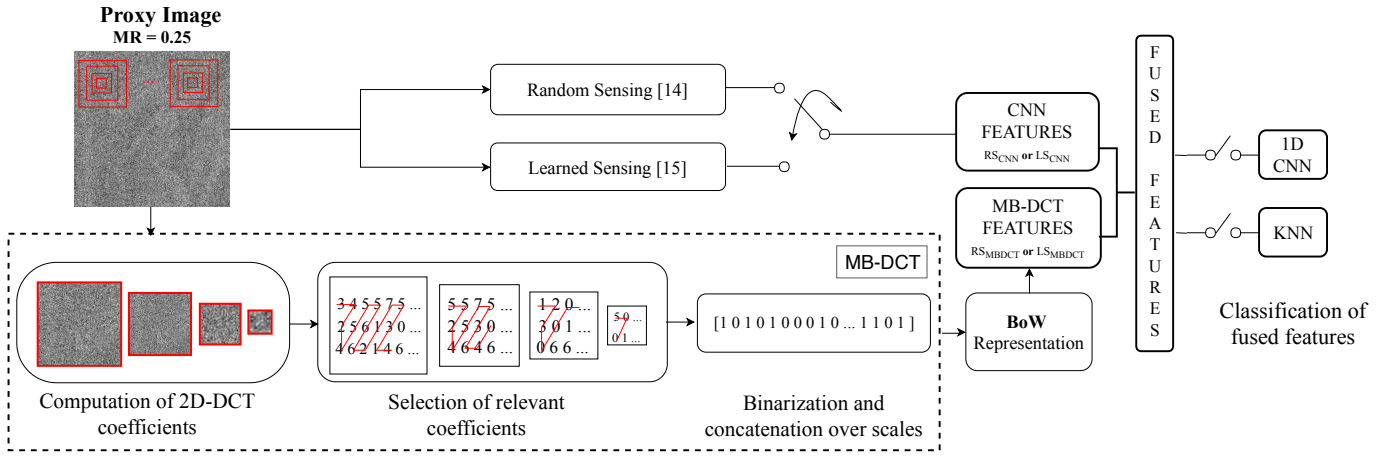


Fig. 3: Computational pipeline for the proposed approach.

mean quantization provide slightly better results (around 0.5% improvement).

(4) *Concatenation of different scales*: The final binary descriptor for a given keypoint is obtained by concatenation of binarized DCT coefficient sets at each scale.

The computational pipeline of the MB-DCT scheme is illustrated in Figure 3.

B. Performance of MB-DCT features for classification of CS proxies

We first compute MB-DCT features densely on the CS proxies of input images as in Eq. 4. Then, we extract image descriptors from these features according to the two schemes explained in the sequel.

1) *MB-DCT in the BoW framework*: In this scheme, we follow the conventional BoW procedure to compute descriptors of CS proxies. We learn a visual dictionary by K-Means clustering of dense MB-DCT features using hamming distance and computed on a training image set. The MB-DCT feature of each image point is assigned the nearest binary descriptor from the dictionary with hard voting. Finally, we apply average pooling to compute a single image signature to obtain the BoW representation of each image.

2) *Fusion of MB-DCT with Deep Learning features*: Deep learning approaches have been shown to provide superior performance in the solution of inference problems provided sufficient amount of training data is available. Nevertheless, recent studies have demonstrated that the joint use of learned

features and hand-crafted features (e.g., MB-DCT) can result in improved performance [23], [24].

For this purpose, we have jointly used the BoW descriptors obtained from MB-DCT features with CNN features computed as in the two recent works, i.e. [14] and [15]. In both cases, proxy images are recovered by pre-multiplying the CSM vector with the transpose of the sensing matrix. In [14], the sensing matrix consists of random Gaussian numbers while in *Compressive Learning (CL)* the sensing matrix is obtained using a deep learning architecture. In both approaches, CNN features are computed on the proxy images. This procedure of MB-DCT and CNN features is shown in the two upper branches of the block diagram in Figure 3. We have named the CNN-derived feature scheme in [14] as *Random Sensing + CNN* (shortly RS_{CNN}) and that in [15] as *Learned Sensing + CNN* (shortly LS_{CNN}), respectively.

Some examples of proxy images recovered with the transpose of the random Gaussian matrix using Eq. 4 are shown in Figure 4 for four sampling rates. Starting from such a proxy image, we compute CNN features (coefficients of the fully connected last layer) using the Lenet5 model [14]. We also compute in parallel BoW descriptors from MB-DCT features, and we refer to this method as RS_{MB-DCT} . Finally, after L_2 normalization, separately of each descriptor, we concatenate them to obtain the joint descriptor. We denote the fused descriptor as $RS_{(CNN|MB-DCT)}$.

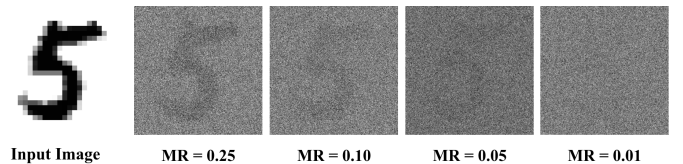


Fig. 4: Proxy images recovered when random sensing is used at different sensing rate

TABLE I: Effect of the quantity of DCT coefficients, as a function of energy preserved, on classification performance of MNIST proxy images at different measurement rates.

Measurement Rate	90% Energy	95% Energy	100% Energy
0.25	8.75	8.67	7.26
0.10	10.81	10.57	9.49
0.05	16.04	15.21	14.28
0.01	41.99	41.1	41.33

For the LS_{CNN} algorithm [15], we learned the sampling matrix for the MNIST dataset, i.e. we get the Ψ and Ψ^T matrices in Eq. 4 from the first and second fully connected

TABLE II: Test error rates on MNIST dataset. MR: Measurement Rate; RS: Random Sensing; LS: Learned Sensing, [†] denotes our re-implementation of [14] and [15]; [*] denotes our proposed features. Presented results are obtained with the KNN classifier.

MR	Smashed Filter [9]	RS_{CNN} [14]	RS_{CNN}^\dagger	RS_{MBDCT}^*	$RS_{(CNN MBDCT)}^*$	LS_{CNN} [15]	LS_{CNN}^\dagger	LS_{MBDCT}^*	$LS_{(CNN MBDCT)}^*$
0.25	27.42%	1.63%	1.73%	7.26%	2.17%	1.56%	1.95%	5.84%	1.58%
0.10	43.55%	2.99%	2.98%	9.46%	3.02%	1.91%	1.88%	5.90%	1.58%
0.05	53.21%	5.18%	4.78%	14.28%	4.44%	2.86%	2.12%	5.80%	1.59%
0.01	63.03%	41.06%	45.8%	41.33%	24.78%	6.46%	5.52%	19.88%	3.87%

TABLE III: Test error rates of the proposed features on MNIST dataset obtained with different classifiers

Measurement Rate	RS_{MBDCT}		$RS_{(CNN MBDCT)}$		LS_{MBDCT}		$LS_{(CNN MBDCT)}$	
	KNN	1D-CNN	KNN	1D-CNN	KNN	1D-CNN	KNN	1D-CNN
0.25	7.26%	8.37%	2.17%	1.69%	5.84%	5.88%	1.58%	1.58%
0.10	9.46%	10.01%	3.02%	2.87%	5.90%	6.19%	1.58%	1.75%
0.05	14.28%	14.16%	4.44%	4.66%	5.80%	5.64%	1.59%	1.63%
0.1	41.33%	48.42%	24.78%	28.11%	19.88%	21.09%	3.87%	4.57%

layers of the trained network. We compute BoW representation of MB-DCT features on these proxies referred to as LS_{MB-DCT} . Similarly, we get the CNN features from the last fully connected layer of the network. Finally, applying L_2 normalization to each, we concatenate them to obtain the joint features that we name as $LS_{(CNN|MB-DCT)}$.

IV. PERFORMANCE EVALUATION

A. Experimental setup

We have experimented on the MNIST dataset that contains hand-written digit images and we followed the same experimental setup in [14] as 50K and following 10K images are used in training and testing, respectively.

a) *Computation of the features:* To compute MB-DCT features, we learned a visual dictionary by K-means clustering based on hamming distance and using training set consisting of 100 randomly selected proxy images. We worked with K=512 clusters as in [16]. The following procedures are as mentioned in Section IV.B.1.

In order to compute RS_{CNN} and LS_{CNN} features we have re-implemented the corresponding architectures in [14] and [15] using the Keras library. For the RS_{CNN} case, we have trained the network in [14] using stochastic gradient descent with the parameters: learning rate 0.01, momentum 0.9, weight decay 0.0005, and we applied 15K epochs following [14]. For the implementation of LS_{CNN} we have trained the network in [15] with Adam optimizer, using learning rate 0.00025 and 500 epochs. Training took around 60 (due to high number of epochs) and 2 hours for the techniques of RS_{CNN} and LS_{CNN} , respectively, with the GPU of GTX 1080 Ti.

b) *Choice of the classifier:* We ran experiments with two different classifiers, namely, KNN and 1D-CNN. For KNN, we used the chi-square distance to compare histograms. We decided for the best value of 'k' by 5-fold cross-validation on the training set and then measured the performance on the test set.

We further wanted to examine the classification performance with a multilayer neural network. However, since the length of the features were quite high, i.e., 1012 for RS_{CNN} and

596 for LS_{CNN} (recall that these are also to be augmented with the 512 dimensional MB-DCT features in the fusion scheme), we decided not to follow this path to avoid excessive computational overhead. Instead we opted to train a 1D-CNN network, adopting Lenet-5 model, with the computed features of the training images. We used Adam optimizer with a learning rate of 0.00025 and 500 epochs in training which took around 2 hours for all the techniques.

B. Performance results

The performance results that are obtained with the aforementioned techniques in terms of test error are presented at Table II. We also present three published performance results in the literature, namely, Smashed Filter [9], RS_{CNN} [14] and LS_{CNN} [15].

We observe that with our re-implementation of RS_{CNN} and LS_{CNN} , we get performances quite close to the reported ones in [14] and [15]. For the degraded proxy image with random sampling, our binary descriptor (RS_{MB-DCT}) outperforms Smashed Filters [9] significantly. RS_{MB-DCT} also gives competitive results with respect to RS_{CNN} [14] for the lowest measurement rate (0.01). We outperform RS_{CNN} [14] at the lowest measurement rate significantly when we use the fused feature (41.06% vs 24.78%).

The significant performance gain is achieved when degradation is created by the learned matrices. In that case, although LS_{MB-DCT} was behind the reported LS_{CNN} results in [15], our re-implementation of LS_{CNN} was slightly better than theirs. More significantly, lowest classification error rates which can be accepted as the new state-of-the-art are obtained when we use joint features in $LS_{(CNN|MB-DCT)}$ implementation (3.87% test error for 0.01 measurement rate).

The performance results presented in Table II are obtained with the KNN classifier. We also present the performance results obtained with 1D-CNN at Table III. As it can be seen in Table III, although they were competitive for higher sampling rates, KNN always gives better result, more significantly at lowest measurement rate. However, execution time of KNN

classifier was much higher than the 1D-CNN execution time on GPU.

V. CONCLUSION

In this work, we proposed a DCT-based discriminative feature scheme, computed directly from the proxy image which is usually a heavily degraded version of the original image. This feature vector (called MB-DCT) is binary, hence simple and low cost. We further introduced feature fusion by concatenating Bag of Words (BoW) representation of our binary features with one of the two state-of-the-art CNN-based feature vectors. Our experimental results show that proposed scheme gives the state-of-the-art performance for compressively sensed image classification even at the lowest measurement rate.

REFERENCES

- [1] E. J. Candès *et al.*, “Compressive sampling,” in *Proceedings of the international congress of mathematicians*, vol. 3, pp. 1433–1452, Madrid, Spain, 2006.
- [2] T. Wimalajeewa, H. Chen, and P. K. Varshney, “Performance limits of compressive sensing-based signal classification,” *IEEE Transactions on Signal Processing*, vol. 60, no. 6, pp. 2758–2770, 2012.
- [3] J. Haupt, R. Castro, R. Nowak, G. Fudge, and A. Yeh, “Compressive sampling for signal classification,” in *Signals, Systems and Computers, 2006. ACSSC’06. Fortieth Asilomar Conference on*, pp. 1430–1434, IEEE, 2006.
- [4] M. A. Davenport, P. T. Boufounos, M. B. Wakin, and R. G. Baraniuk, “Signal processing with compressive measurements,” *IEEE Journal of Selected Topics in Signal Processing*, vol. 4, no. 2, pp. 445–460, 2010.
- [5] R. Calderbank, S. Jafarpour, and R. Schapire, “Compressed learning: Universal sparse dimensionality reduction and learning in the measurement domain,” *preprint*, 2009.
- [6] M. A. Davenport, M. F. Duarte, M. B. Wakin, J. N. Laska, D. Takhar, K. F. Kelly, and R. G. Baraniuk, “The smashed filter for compressive classification and target recognition,” in *Computational Imaging V*, vol. 6498, p. 64980H, International Society for Optics and Photonics, 2007.
- [7] W. B. Johnson and J. Lindenstrauss, “Extensions of lipschitz mappings into a hilbert space,” *Contemporary mathematics*, vol. 26, no. 189-206, p. 1, 1984.
- [8] K. Kulkarni and P. Turaga, “Reconstruction-free action inference from compressive imagers,” *IEEE transactions on pattern analysis and machine intelligence*, vol. 38, no. 4, pp. 772–784, 2016.
- [9] S. Lohit, K. Kulkarni, P. Turaga, J. Wang, and A. C. Sankaranarayanan, “Reconstruction-free inference on compressive measurements,” in *Proceedings of the IEEE Conference on Computer Vision and Pattern Recognition Workshops*, pp. 16–24, 2015.
- [10] M. Shoaib, N. K. Jha, and N. Verma, “Signal processing with direct computations on compressively sensed data,” *IEEE Transactions on Very Large Scale Integration (VLSI) Systems*, vol. 23, no. 1, pp. 30–43, 2015.
- [11] S. Chen, W. Hua, Z. Li, J. Li, and X. Gao, “Heartbeat classification using projected and dynamic features of ecg signal,” *Biomedical Signal Processing and Control*, vol. 31, pp. 165–173, 2017.
- [12] A. Kabán, “New bounds on compressive linear least squares regression,” in *Artificial Intelligence and Statistics*, pp. 448–456, 2014.
- [13] R. J. Durrant and A. Kabán, “Compressed fisher linear discriminant analysis: Classification of randomly projected data,” in *Proceedings of the 16th ACM SIGKDD international conference on Knowledge discovery and data mining*, pp. 1119–1128, ACM, 2010.
- [14] S. Lohit, K. Kulkarni, and P. Turaga, “Direct inference on compressive measurements using convolutional neural networks,” in *Image Processing (ICIP), 2016 IEEE International Conference on*, pp. 1913–1917, IEEE, 2016.
- [15] A. Adler, M. Elad, and M. Zibulevsky, “Compressed learning: A deep neural network approach,” *arXiv preprint arXiv:1610.09615*, 2016.
- [16] S. Aslan, M. Yamaç, and B. Sankur, “A dct-based multiscale binary descriptor robust to complex brightness changes,” in *Signal Processing Conference (EUSIPCO), 2016 24th European*, pp. 1573–1577, IEEE, 2016.
- [17] D. L. Donoho and M. Elad, “Optimally sparse representation in general (nonorthogonal) dictionaries via l_1 minimization,” *Proceedings of the National Academy of Sciences*, vol. 100, no. 5, pp. 2197–2202, 2003.
- [18] J. A. Tropp, “Just relax: Convex programming methods for identifying sparse signals in noise,” *IEEE transactions on information theory*, vol. 52, no. 3, pp. 1030–1051, 2006.
- [19] A. Mousavi and R. G. Baraniuk, “Learning to invert: Signal recovery via deep convolutional networks,” in *Acoustics, Speech and Signal Processing (ICASSP), 2017 IEEE International Conference on*, pp. 2272–2276, IEEE, 2017.
- [20] S. Lohit, K. Kulkarni, R. Kerviche, P. Turaga, and A. Ashok, “Convolutional neural networks for non-iterative reconstruction of compressively sensed images,” *arXiv preprint arXiv:1708.04669*, 2017.
- [21] C. A. Metzler, A. Maleki, and R. G. Baraniuk, “From denoising to compressed sensing,” *IEEE Transactions on Information Theory*, vol. 62, no. 9, pp. 5117–5144, 2016.
- [22] E. J. Candès, “The restricted isometry property and its implications for compressed sensing,” *Comptes rendus mathématique*, vol. 346, no. 9-10, pp. 589–592, 2008.
- [23] E. G. Danaci and N. Ikizler-Cinbis, “Low-level features for visual attribute recognition: An evaluation,” *Pattern Recognition Letters*, vol. 84, pp. 185–191, 2016.
- [24] S. Aslan, C. B. Akgül, B. Sankur, and E. T. Tunali, “Exploring visual dictionaries: a model driven perspective,” *Journal of Visual Communication and Image Representation*, vol. 49, pp. 315–331, 2017.